の増加あるいは維持が目的となり，現在は骨折予防ができなければ，骨粗鬆症の治療ではないと考えられるようになってきた．逆にいえば，骨代謝に何の影響を与えられなくとも，骨折を予防することができれば目標は達成したことになる．実際，多くの運動プログラムが転倒を予防するのに有効であることが示されており[15]，そういう方向で運動療法をとらえて行くべきではないかと私は考えている．

運動療法と骨代謝の関係を調べてきた研究の多くは，骨量・骨量にあまりにも注目しすぎてきたのではないだろうか．その理由は，それが最も調べやすかったからであり，本当の調査対象は別のところにあったと考えている．

■文　献

1) Heinonen A, et al: Bone mineral density in female athletes representing sports with different loading characteristics of the skeleton. Bone **17**: 197-203, 1995.
2) Morel J, et al: Bone mineral density of 704 amateur sportsmen involved in different physical activities. Osteoporos Int **12**: 152-157, 2001.
3) Bass S, et al: Exercise before puberty may confer residual benefits in bone density in adulthood: studies in active prepubertal and retired female gymnasts. J Bone Miner Res **13**: 500-507, 1998.
4) Bailey DA, et al: A six-year longitudinal study of the relationship of physical activity to bone mineral accrual in growing children: the university of Saskatchewan bone mineral accrual study. J Bone Miner Res **14**: 1672-1679, 1999.
5) Kelley GA, et al: Resistance training and bone mineral density in women: a meta-analysis of controlled trials. Am J Phys Med Rehabil **80**: 65-77, 2001.
6) Wallace BA, Cumming RG: Systematic review of randomized trials of the effect of exercise on bone mass in pre- and postmenopausal women. Calcif Tissue Int **67**: 10-18, 2000.
7) Cavanaugh DJ, Cann CE: Brisk walking does not stop bone loss in postmenopausal women. Bone **9**: 201-204, 1988.
8) Jones PR, et al: Influence of brisk walking on the broadband ultrasonic attenuation of the calcaneus in previously sedentary women aged 30-61 years. Calcif Tissue Int **49**: 112-115, 1991.
9) Brooke-Wavell K, et al: Brisk walking reduces calcaneal bone loss in post-menopausal women. Clin Sci(Lond) **92**: 75-80, 1997.
10) Ebrahim S, et al: Randomized placebo-controlled trial of brisk walking in the prevention of postmenopausal osteoporosis. Age Ageing **26**: 253-260, 1997.
11) Zanker CL, Swaine IL: Responses of bone turnover markers to repeated endurance running in humans under conditions of energy balance or energy restriction. Eur J Appl Physiol **83**: 434-440, 2000.
12) Rudberg A, et al: Serum isoforms of bone alkaline phosphatase increase during physical exercise in women. Calcif Tissue Int **66**: 342-347, 2000.
13) Valentino R, et al: The influence of intense ballet training on trabecular bone mass, hormone status, and gonadotropin structure in young women. J Clin Endocrinol Metab **86**: 4674-4678, 2001.
14) Creighton DL, et al: Weight-bearing exercise and markers of bone turnover in female athletes. J Appl Physiol **90**: 565-570, 2001.
15) Carter ND, et al: Exercise in the prevention of falls in older people: a systematic literature review examining the rationale and the evidence. Sports Med **31**: 427-438, 2001.

Mod Rheumatol (2004) 14:399–401
DOI 10.1007/s10165-004-0330-5

CASE REPORT

Kentaro Inui · Takafumi Maeno · Masahiro Tada
Kunio Takaoka · Tatsuya Koike

Open reduction of the dislocated hip in juvenile idiopathic arthritis: a case report

Received: December 23, 2003 / Accepted: May 25, 2004

Abstract An 8-year-old girl with systemic-onset juvenile idiopathic arthritis (JIA) required surgical reduction for a dislocated left hip joint following failure of skin traction for 1 week. Unaided walking was achieved by 3 months postoperatively. Incongruence and irregularity of the hip joint remained but may resolve with maturation. Joint laxity caused by synovitis, flexion/adduction contracture with pain, and acetabular dysplasia by growth disturbance apparently caused hip dislocation.

Key words Hip dislocation · Juvenile idiopathic arthritis (JIA) · Surgical reduction

Introduction

Systemic-onset juvenile idiopathic arthritis (JIA) is difficult to treat and can eventually become indistinguishable from polyarticular-onset JIA.[1] Systemic- or polyarticular-onset JIA results in severe destruction of polyarticulation, including hip joints. As hip joint involvement can cause severe residual disability, treatment of this joint is extremely important for preserving the quality of life in young patients. The present article describes a rare case of dislocated hip joint in a patient with JIA for which surgical reduction was performed.

Case reports

A 3-year-old girl experienced high fever, spiking at 37°–39°C. Ultrasonographic examination showed no hepatosplenomegaly. High fever recurred several times annually until the patient was 8 years old, and JIA was diagnosed. There had been no use of corticosteroids or disease-modifying antirheumatic drugs (DMARDs). At 8 years of age she developed polyarthralgia in both hip joints and visited a hospital. Nonsteroidal antiinflammatory drugs were prescribed and a rehabilitation program was initiated to restore range of motion (ROM) in several joints. Four months later, leg-length discrepancy became apparent, and posterior dislocation of the left hip was revealed on radiography. The patient was then referred to our hospital.

Physical examination

Her body weight was 16.1 kg (−2.3 SD), and her height was 120 cm (−1.6 SD). The patient displayed eight painful joints (both wrists, hips, and knee and ankle joints), but only the bilateral knee joints were swollen. Neither skin rash nor uveitis was detected on her first visit to our hospital. Her left hip joint was contracted in flexion, adduction, and internal rotation, with severe pain. A leg-length discrepancy of 8 cm was apparent, and a small spherical bony prominence was palpable on her left buttock. Both wrists and both ankle joints were also contracted.

Laboratory findings

Blood counts were normal, but severely high levels of C-reactive protein were identified (9.9 mg/dl). The erythrocyte sedimentation rate was 90 mm/h. The negative rheumatoid factor, negative antinuclear antibody, and HLA-DR4 indicated systemic-onset JIA.

Imaging findings

Radiography revealed posterior dislocation of the left hip joint with severe osteopenia (Fig. 1A). However, destruction of the joint surface was not evident, and no destructive changes were detected on radiographs of other joints. Bilateral acetabula were dysplastic, and growth plates were

K Inui · T. Maeno · M. Tada · K Takaoka · T Koike (✉)
Department of Orthopaedic Surgery, Osaka City University Medical School, 1-4-3 Asahi-machi, Abeno-ku, Osaka 545-8585, Japan
Tel. +81-6-6645-3851; Fax +81-6-6646-6260
e-mail: tatsuya@med.osaka-cu.ac.jp

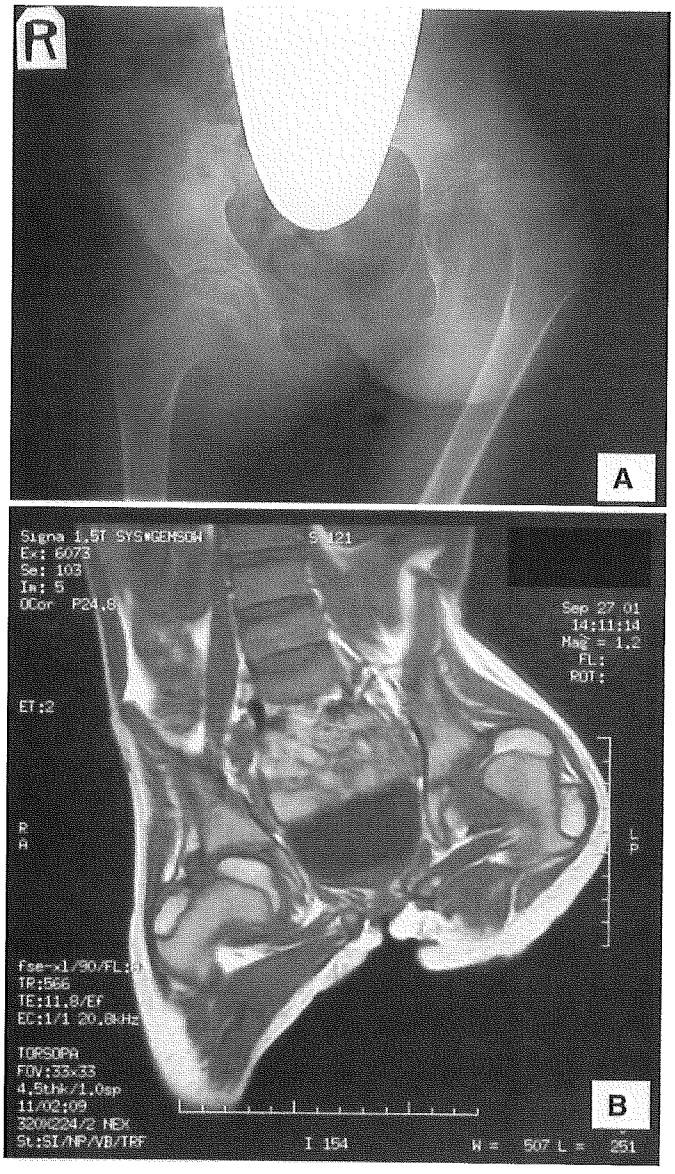

Fig. 1. Affected hip joint at first visit. **A** Radiography revealed severe osteoporosis with a dislocated left hip joint in addition to acetabular dysplasia. **B** Magnetic resonance imaging indicated normal intensity of the femoral head, suggesting the absence of idiopathic osteonecrosis

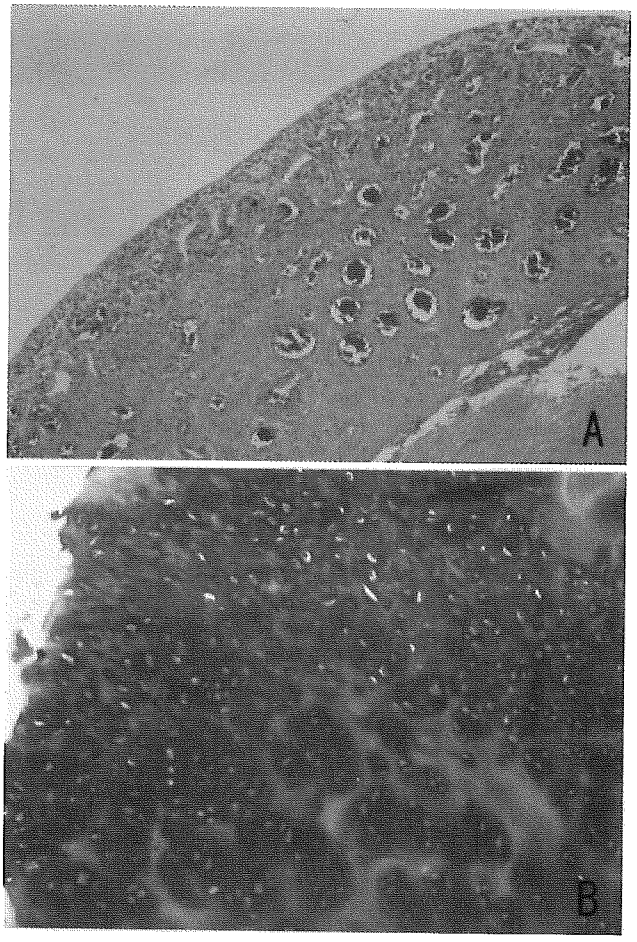

Fig. 2. Histological examination of tissue obtained from the affected hip joint at surgery. **A** Hypertrophic synovium was observed with proliferated and dilated vessels (×200). **B** Inside of joint displayed irregularity of the articular surfaces and numerous scattered cartilage fragments. Articular cartilage was severely degenerated (×400)

nearly closed. T2-weighted magnetic resonance imaging (MRI) indicated that avascular necrosis of the femoral head had not occurred (Fig. 1B).

Surgical treatment and postoperative course

Skin traction of the left limb for 1 week proved unsuccessful, so open reduction of the dislocated hip joint was performed. Using an anterolateral approach, and taking extreme care to avoid damaging the vascular structures to the femoral head, the affected hip joint filled with copious synovia was observed. An irregular articular surface of the acetabulum was seen, with numerous small fragments of cartilage in the joint cavity. Reduction of the femoral head was achieved after resecting the iliopsoas and adductor muscle tendons. Synovectomy of the affected joint was also performed. Histological examination revealed multiple cell layers with proliferated vessels in the synovium and severely degenerated articular cartilage (Fig. 2). A hip spica cast was applied for 3 weeks in the frog-leg position followed by 3 weeks in the functional position. Although the hip joint was considered at risk of spontaneous fusion, the reduced position was maintained with preservation of the ROM (Fig. 3). After removing the cast, standing and gait exercises were initiated using a long leg brace and crutches, as well as prescription of methotrexate, salazosulfapyridine, and glucocorticoid. The patient was able to walk unaided and independently by 3 months after the operation.

Discussion

In general, JIA leads to joint inflammation and growth disturbance. The former causes destruction of the articular cartilage and joint subluxation, and the latter causes loss

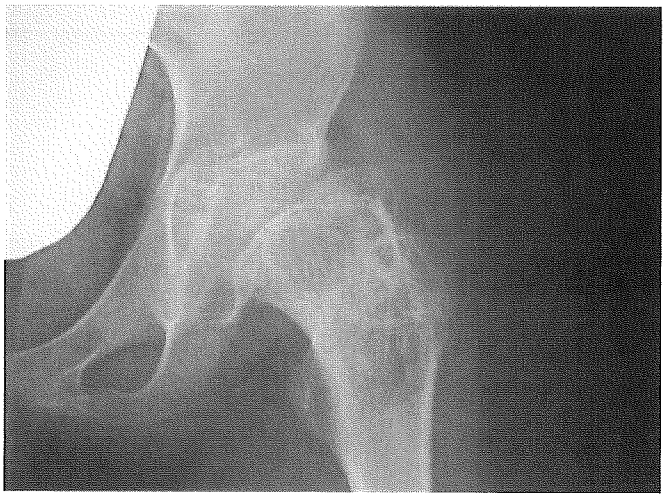

Fig. 3. Radiograph at the final follow-up. The reduced position was maintained, but joint congruence was not recovered

of congruence in the joint. Hip joints reportedly display several forms of destruction, including an Otto pelvis, subluxation, dysplastic hip, deformity of the femoral head or combinations of these problems. The ratio of hip involvement is reportedly 70% in JIA[2] and 50% in systemic JIA.[3] In most cases, hips display subluxation or central migration.[4]

Dislocation of the hip in JIA is rare, and to the best of our knowledge this is only the second report of such a case.[5] In this case, joint laxity caused by synovitis, flexion/adduction contracture with pain, and acetabular dysplasia due to growth disturbance contributed to dislocation of the hip joint.

The dislocated hip should be reduced by any means. In the first report in 1975,[5] the hip was successfully reduced using skin traction and subsequent cast immobilization. Once reduced, hip joint remodeling can be expected in the best-case scenario because of the young age of the patients, such as in the case reported in 2000.[6] If the best-case scenario does not occur, spontaneous ankylosing or severe destruction of the hip joint occurs, often leading to significant functional disability and subsequent joint replacement, even in young patients. At final follow-up, this girl was able to walk unaided, but radiography revealed inappropriate congruity with severe dysplasia of the acetabulum and deformation of the femoral head. Additional surgical treatment will probably be necessary in the future for her hip joint so she can have a normal social and school life, as do approximately 80% of children in Japan with systemic or polyarticular JIA.[7]

References

1. Ilowite NT. Current treatment of juvenile rheumatoid arthritis. Pediatrics 2002;109:109–15.
2. Cooperman D, Emery H, Keller C. Factors relating to hip joint arthritis following three childhood diseases: juvenile rheumatoid arthritis, Perthes disease, and postreduction avascular necrosis in congenital hip dislocation. J Pediatr Orthop 1986;6:706–12.
3. Svantesson H, Akesson A, Eberhardt K, Elborgh R. Prognosis in juvenile rheumatoid arthritis with systemic onset: a follow-up study. Scand J Rheumatol 1983;12:139–44.
4. Laxer RM, Schneider R, Woo P, Glass DN. Systemic-onset juvenile chronic arthritis. In: Maddison PJ, Isenberg DA, editors. Oxford textbook of rheumatology. 2nd edn. Oxford: Oxford University Press; 1998. p. 1114–31.
5. Ahmad I. Juvenile rheumatoid arthritis causing hip dislocation: case report. Bull Hosp Joint Dis 1975;36:159–62.
6. Banks S, Ostrov BE. Clinical images: hip joint remodeling in systemic-onset juvenile rheumatoid arthritis. Arthritis Rheum 2000;43:2856.
7. Fujikawa S, Okuni M. Clinical analysis of 570 cases with juvenile rheumatoid arthritis: results of a nationwide retrospective survey in Japan. Acta Paediatr Jpn 1997;39:245–9.

カレントテラピー

別刷

月刊カレントテラピー［別刷］2004 VOL.22 NO.3 3月号

治療薬としてのPTH

小池達也*

abstract

副甲状腺ホルモン（PTH）は，骨形成作用を有する骨粗鬆症治療薬であり，骨折閾値以下にまで低下した骨塩量を増加させうる能力を有している．大規模臨床試験で，骨塩量の増加および脊椎圧迫骨折や非脊椎骨折の予防効果があることが証明されており，米国では2002年より，骨粗鬆症治療薬として認可されている．さらに，ステロイド性の骨粗鬆症や男性の骨粗鬆症に対しても骨塩量増加をエンドポイントとして，その効果が確認されている．ただし，皮質骨量に対する作用は十分ではない．

おもしろいことに，PTH治療に引き続くビスフォスフォネート治療は治療効果が相加されるが，併用療法では単独療法以上の効果は期待できない．動物実験において，高用量長期のPTH投与により骨肉腫の発生を認めたため，治験は一時中止されていた．しかし，今後再開の見通しが立ち，その場合には海外の標準である連日皮下投与ではない方法が採用される可能性が高い．

I はじめに

現在の骨粗鬆症治療薬は，ビスフォスフォネート・カルシトニン・女性ホルモンなど骨吸収抑制剤が主流である．代表的薬剤であるビスフォスフォネートは，強力に骨吸収を抑制し，骨塩量を増加させる．しかし，その増加は初年度には著明であるが，その後の増加には鈍化傾向が認められる．これまでの大規模臨床試験[1]の報告でも，3年で10%程度の増加にとどまる．

したがって，骨折閾値以下まで低下した骨量を増加させうる骨形成促進剤は非常に魅力的な存在である．副甲状腺ホルモン（PTH）は，骨形成を促進し骨量を増加させることが知られており[2]，米国では2002年に骨粗鬆症治療薬として認可されている．

II PTHが骨量に与える影響

Finkelsteinら[3]は，子宮内膜症の治療のためにGnRHアゴニストの投与を受け偽閉経状態となった女性患者を無作為に2群に分け，一方にヒトPTH（hPTH）（1-34）の40μg連日皮下投与を行った．その結果，PTH非投与群では12カ月で4～5%の骨塩量低下が腰椎・大腿骨に認められ，全身骨塩量でも2%の低下が認められた．ところが，同時にPTHを投与された群では，腰椎で逆に2%の骨塩量増加を認め，大腿骨では治療6カ月の時点まではPTH非投与群と同様に減少傾向が認められたが，12カ月時点では開始時の骨塩量に復していた．

* 大阪市立大学大学院医学研究科リウマチ外科学　助教授

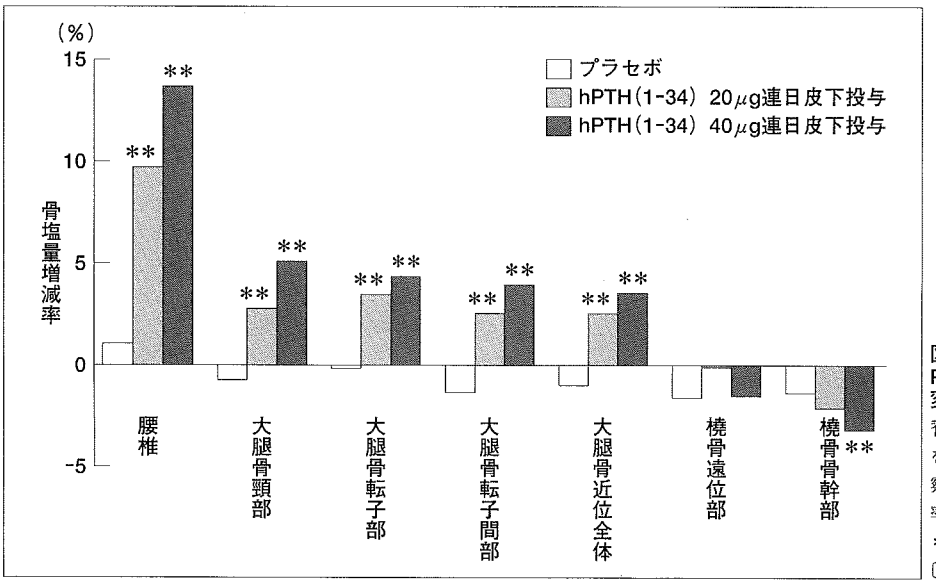

図1
PTH投与後の身体部位別骨塩量変化率
脊椎圧迫骨折を有する閉経後女性を各群500名前後で平均21カ月の観察．開始時の骨塩量に対する変化率で表示．
**：$p<0.001$ vs プラセボ
〔文献4)の表より作成〕

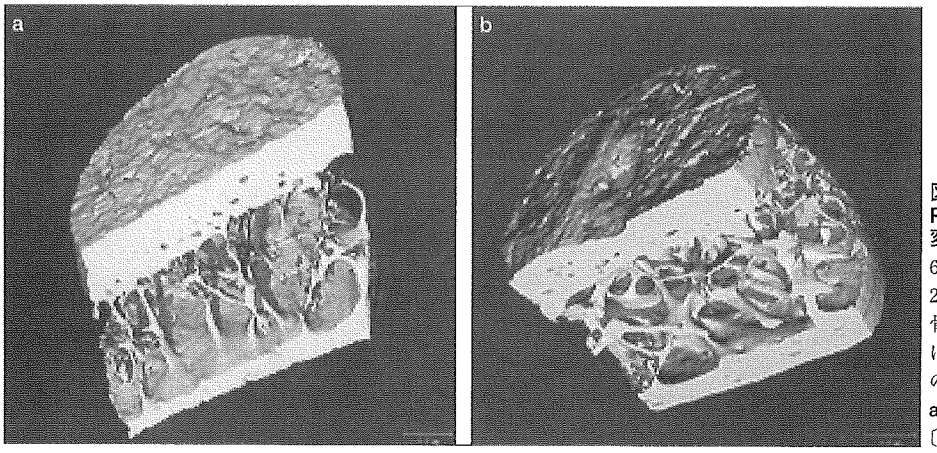

図2
PTH投与前後の腸骨骨梁構造の変化
65歳の女性にテリパラチド20μgを21カ月間投与し，投与前後で腸骨骨生検を行い，3Dμ CTイメージに再構築した．骨梁幅や皮質骨との連結を観察することができる．
a：投与前，b：投与後
〔文献8)より引用〕

この結果は，PTH投与が閉経後骨粗鬆症の治療薬として非常に有望であることを示している．実際その後に，Finkelsteinの同僚であるNeerを中心に行われた大規模臨床試験[4]により，その効果は確認された．彼らは1,637名の脊椎圧迫骨折を有する閉経後女性を3群に分け，1群にはプラセボを，残り2群にはhPTH(1-34)の20あるいは40μg連日皮下投与を平均21カ月間行った．40μg投与群では腰椎で13.7%，大腿骨頸部でも5.1%の増加を認めた．**図1**に示すように他の部位でも，有意な骨塩量増加が認められたが，橈骨骨幹部においては逆にPTH投与群で有意な減少を認めた．

PTH投与は，閉経後骨粗鬆症に限らず，ステロイド性骨粗鬆症[5]や男性における骨粗鬆症[6]に対しても有意な骨塩量増加をもたらした．これら海外でのPTHの投与方法は，すべて連日の自己皮下投与であるが，わが国での臨床研究では別の投与方法が採用された．Fujitaら[7]は，骨粗鬆症女性220例に対して，hPTH(1-34)（50，100，200U）を週1回の皮下注で投与し，1年後に最大用量群で腰椎骨塩量が8.1%増加したと報告している．

Ⅲ PTHが皮質骨および骨構造に与える影響

先に述べたNeerらの研究[4]では，橈骨骨幹部の骨塩量はPTHの投与により逆に減少を示した．他の研究[3),5)~7)]でも，PTHの投与により橈骨骨幹部

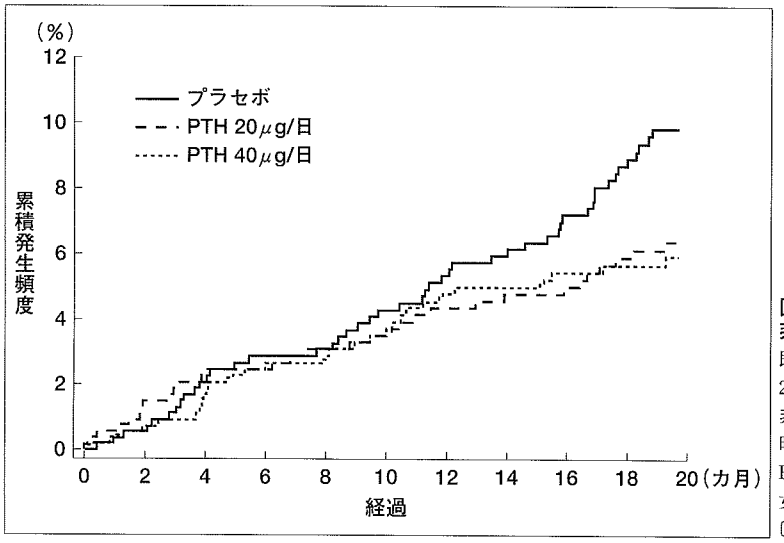

図3
非脊椎骨折の累積発生頻度
既存脊椎骨折を有する女性を3群（プラセボ，PTH 20μg/日，PTH 40μg/日）に分け，20カ月間追跡し，非脊椎骨折を起こした症例の累積割合を示す．開始時には3群間に差を認めないが，9～12カ月後にはPTH投与群よりもプラセボ群で非脊椎骨折を有する女性の割合が増加した．
〔文献4)より引用改変〕

などの皮質骨骨塩量を増加しうるという証拠は得られていない．これはおそらく，まず皮質骨の代謝が促進され，海綿骨の骨塩量増加の基礎になっているためだと考えられている．

一方，PTH投与後の骨梁構造変化に関しては，骨生検を用いた最近の報告[8]がある．Jiangらは，51人の脊椎圧迫骨折を有する閉経後5年以上を経過した女性に対して，無作為にテリパラチド〔rhPTH(1-34)〕の連日自己皮下投与を行った．群分けは，プラセボ（n＝19），PTH 20μg（n＝18），PTH 40μg（n＝14）であり，各症例において投与前後に腸骨骨生検を行った．PTH投与群では，**図2**で明らかなように海綿骨の容積・海綿骨間の結合性・皮質骨幅の増大が認められた．この図からも明らかなように，皮質骨に対するPTHの効果はそれほど強力ではない．

Ⅳ PTHの骨折抑制効果

骨塩量は確かに増加するが，骨折抑制に関する効果はどうであろうか．最も大きな臨床試験[4]では，1つ以上の新脊椎圧迫骨折発生率がPTH投与群で，65(20μg群)～69(40μg群)%抑制された．また，非脊椎骨折の累積発生頻度においても，PTH投与群では40%の抑制が認められた（**図3**）．ホルモン補充療法（HRT）をすでに受けている閉経後骨粗鬆症患者にPTHを3年間投与した場合にも，脊椎圧迫骨折は非投与群と比較して有意に抑制された[9]．

Ⅴ PTHとビスフォスフォネート

ともに強力な骨量増加作用を示すPTHとビスフォスフォネートであるが，どちらがより強力なのであろうか．Bodyら[10]は，この2つの薬剤の効果を閉経後骨粗鬆症患者を対象として，同一臨床試験において二重盲検にて比較した．その結果，PTH（テリパラチド40μg連日皮下投与）は，腰椎・大腿骨頸部・全身の骨塩量をビスフォスフォネート（アレンドロネート10mg/日）よりも有意に増加させ，非椎体骨折の発生抑制効果もアレンドロネートより優れていた．ただし，橈骨遠位1/3骨塩量はアレンドロネートに比較して有意に低下した．

2剤を連続して投与すれば，その効果は増加するであろうか，あるいは減弱されるであろうか．Rittmasterら[11]の結果を**図4**に示す．まず，PTH〔rhPTH(1-84) 50～100μg連日皮下〕投与により，1年で腰椎骨塩量は各群平均7.1%の増加を示した(対照群は1.3%)．次の1年は全員に10mg/日のアレンドロネートを投与したところ，1年目にPTH投与を受けた群では平均13.4%の腰椎骨塩量の増加を認め，1年目が対照群であった群は7.1%の増加を示した．この結果から，PTHに引き続きビスフォスフォネートを投与する方法は，単独投与よりもより効

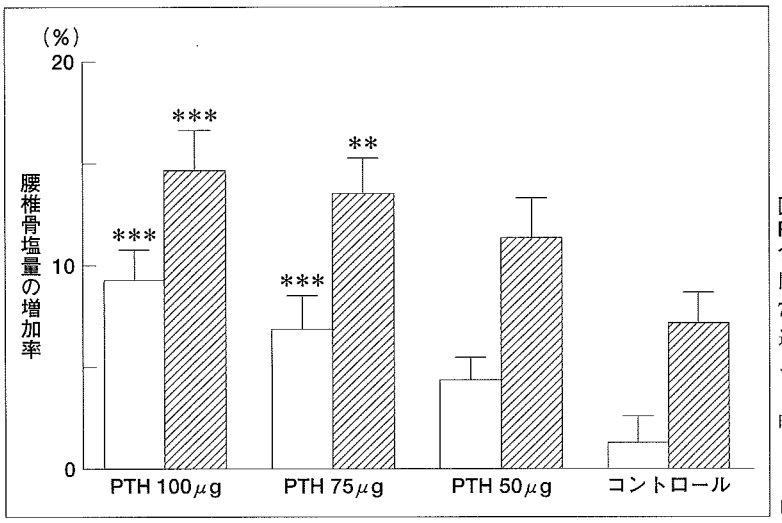

図4
PTHに引き続きアレンドロネートを投与した場合の腰椎骨塩量変化
閉経後骨粗鬆症患者66名を4群〔rhPTH(1-84) 50μg, 75μg, 100μgおよびプラセボ投与〕に分け，1年間経過観察．この時点での腰椎骨塩量増加を白抜きカラムで示す．次の1年はPTH投与を中止し，全員にアレンドロネート10mg/日を投与した．最終（2年後）時点での腰椎骨塩量増加率を斜線カラムで示す．
**：$p<0.01$ vs プラセボ/アレンドロネート群
***：$p<0.001$ vs プラセボ/アレンドロネート群
〔文献11)より引用改変〕

果的であることが判明した．

では，併用療法でも相加的効果を示すであろうか．この命題に挑戦した研究は，2003年の米国骨ミネラル代謝学会でmost outstanding awardを受賞するとともに，すぐにN Engl J Medにて公表された[12]．結果は否定的で，テリパラチドとアレンドロネートの併用は1年の前向き調査で，単独投与群よりも優れてはいなかった．PTH作用が発揮されるには，骨代謝回転が上がる必要があるのかもしれない．

Ⅵ PTHの日本における現状

前述のように，海外でのPTHの投与方法は連日の自己皮下注射が基本である．しかし，わが国では自己注射がなかなか認められないこともあり，臨床試験[7]で採用された週1回の間欠的皮下投与が標準となるものと思われる．

わが国の臨床試験は，その後，ラットへの高用量かつ長期のPTHの投与により，骨肉腫発生頻度が上昇することが判明し，中止された．しかしこの件に関して，米国食品医薬品局（FDA）がヒトにおける治療においては，期間および用量とも当てはまらないと判断し，骨粗鬆症治療薬として認可したため，再びわが国においても臨床試験が計画されている．現時点で3つの企業が臨床治験を予定している．すべてhPTH(1-34)であるが，2社はリコンビナントで残り1社が合成ペプチド．また，投与方法も2社は皮下注射であるが，残り1社は経鼻投与を考えている．骨粗鬆症治療のさらなる進歩はそこまできている．

参考文献

1) Black DM, et al：Randomised trial of effect of alendronate on risk of fracture in women with existing vertebral fractures. Fracture Intervention Trial Research Group. Lancet 348：1535～1541, 1996
2) Dempster DW, et al：Anabolic actions of parathyroid hormone on bone. Endocr Rev 14：690～709, 1993
3) Finkelstein JS, et al：Prevention of estrogen deficiency-related bone loss with human parathyroid hormone-(1-34)：a randomized controlled trial. JAMA 280：1067～1073, 1998
4) Neer RM, et al：Effect of parathyroid hormone (1-34) on fractures and bone mineral density in postmenopausal women with osteoporosis. N Engl J Med 344：1434～1441, 2001
5) Lane NE, et al：Parathyroid hormone treatment can reverse corticosteroid-induced osteoporosis. Results of a randomized controlled clinical trial. J Clin Invest 102：1627～1633, 1998
6) Kurland ES, et al：Parathyroid hormone as a therapy for idiopathic osteoporosis in men：effects on bone mineral density and bone markers. J Clin Endocrinol Metab 85：3069～3076, 2000
7) Fujita T, et al：Effect of an intermittent weekly dose of human parathyroid hormone (1-34) on osteoporosis：a randomized double-masked prospective study using three dose levels. Osteoporos Int 9：296～306, 1999
8) Jiang Y, et al：Recombinant human parathyroid hormone (1-34) [teriparatide] improves both cortical and cancellous bone structure. J Bone Miner Res 18：1932～1941, 2003
9) Lindsay R, et al：Randomised controlled study of effect of parathyroid hormone on vertebral-bone mass and fracture incidence among postmenopausal women on oestrogen with

osteoporosis. Lancet 350 : 550～555, 1997
10) Body JJ, et al : A randomized double-blind trial to compare the efficacy of teriparatide [recombinant human parathyroid hormone (1-34)] with alendronate in postmenopausal women with osteoporosis. J Clin Endocrinol Metab 87 : 4528～4535, 2002
11) Rittmaster RS, et al : Enhancement of bone mass in osteoporotic women with parathyroid hormone followed by alendronate. J Clin Endocrinol Metab 85 : 2129～2134, 2000
12) Black DM, et al : The effects of parathyroid hormone and alendronate alone or in combination in postmenopausal osteoporosis. N Engl J Med 349 : 1207～1215, 2003

ARTHRITIS & RHEUMATISM
Vol. 52, No. 2, February 2005, pp 637–641
DOI 10.1002/art.20794

Use of Local Electroporation Enhances Methotrexate Effects With Minimum Dose in Adjuvant-Induced Arthritis

Masahiro Tada, Kentaro Inui, Tatsuya Koike, and Kunio Takaoka

Objective. **To investigate the effects of electrical pulses on the ability of methotrexate (MTX) to attenuate inflammation and subsequent joint destruction in rats with adjuvant-induced arthritis (AIA).**

Methods. **Rats in the experimental group received an intraperitoneal injection of MTX (0.125 mg/kg body weight), followed 30 minutes later by application of direct electrical pulses (50V, 8 Hz) to their left hind paws with an electroporation apparatus (M+/E+ group; n = 8). The procedure was repeated twice weekly for 3 weeks. Three control groups received the following treatments, respectively: MTX without electrical treatment (M+/E− group; n = 9), electrical treatment but no MTX (M−/E+ group; n = 10), or no electrical treatment and no MTX (M−/E− group; n = 9). Progression of AIA was monitored by joint swelling and radiologic and histologic changes in the ankle joint.**

Results. **Three weeks after injection of the adjuvant, and at the height of the arthritic reaction, the swelling and radiologic and histologic changes in the left hind paws in the M+/E+ rats were significantly reduced, as compared with changes observed in the control groups.**

Conclusion. **These results demonstrate that application of electrical pulses in combination with use of systemic low-dose MTX can ameliorate local arthritic reactions. This response probably occurs because electrical stimulation promotes transient passage of MTX through pores in the cell membranes, with a resultant local increase in the concentration of the drug within the cells. These results point to a potential use of electrochemotherapy to increase the efficacy of MTX or other drugs in an arthritic joint that is refractory to treatment, without increasing the dose of the drug.**

Although new biologic agents (1) can ameliorate inflammatory reactions and consequently protect the joints of patients with rheumatoid disease from progressive damage (2), methotrexate (MTX) remains one of the most effective and widely used disease-modifying antirheumatic drugs (DMARDs) (3). However, chronic inflammation often persists in isolated joints even after effective systemic MTX treatment, presumably as a result of an inadequate concentration of MTX in the joint that is refractory to treatment. In patients with persistent inflammation, synovectomy is often indicated for symptomatic relief, although data on the long-term clinical effectiveness of this approach are limited (4). Another option is an additional dose of MTX, but this increases the risk of adverse events. Because MTX has weak cell permeability, and the pharmacologic effects of this drug depend upon its intracellular concentration, any method for increasing intracellular MTX levels in the joint may be effective in attenuating the inflammatory response.

Electroporation has been used to facilitate the transport of nonpermeable molecules into cells. Transient cell membrane pores, generated electrically, allow nonpermeable molecules, including genes and drugs, to enter into the cells (5). Electroporation systems are now available for clinical use to deliver anticancer drugs into malignant solid tumor cells (6–8) as electrochemotherapy. Encouraging clinical results have been reported for the treatment of malignancies, in terms of efficacy, safety, and cost (9). This suggests that electroporation may be useful for the local treatment of rheumatoid arthritis (RA) that is refractory to conventional therapy.

We used electroporation to enhance the effect of

Supported by the Ministry of Education, Culture, Sports, Science and Technology of Japan (grant-in-aid 15591594).

Masahiro Tada, MD, Kentaro Inui, MD, PhD, Tatsuya Koike, MD, PhD, Kunio Takaoka, MD, PhD: Osaka City University, Graduate School of Medicine, Osaka, Japan.

Address correspondence and reprint requests to Masahiro Tada, MD, Department of Orthopaedic Surgery, Osaka City University, Graduate School of Medicine, 1-4-3 Asahimachi, Abeno-ku, Osaka 545-8585, Japan. E-mail: m-tada@med.osaka-cu.ac.jp.

Submitted for publication May 11, 2004; accepted in revised form October 21, 2004.

low-dose MTX treatment on the progression to severe arthritis and associated joint destruction in a rat model of adjuvant-induced arthritis (AIA) (10–12).

MATERIALS AND METHODS

Animals. Inbred 7-week-old male Lewis rats were purchased from Charles River Japan (Kanagawa, Japan) and housed with free access to standard laboratory chow and water, under 12-hour dark/light cycles in conditioned air.

Induction of arthritis. The adjuvant mixture was prepared by mixing dried heat-killed *Mycobacterium butyricum* (Difco, Detroit, MI) in paraffin oil (Wako, Tokyo, Japan) at a concentration of 5 mg/ml. To induce systemic arthritis, 0.2 ml of the preparation was injected into the tail bases of 8-week-old rats that had received anesthesia via ethyl ether inhalation.

Pulsed electrical stimulation for electroporation. For electrical stimulation to generate transient pores in cell membranes at the target tissue site, we used an electroporation apparatus (CUY-21; Gene System, Osaka, Japan). Direct-current electrical pulses (8 Hz, 75 msec pulse duration, 50 volts/cm electrode distance) of 1-second duration were delivered 6 times during a single procedure. Each of the six 1-second pulses was applied by 2 parallel stainless steel electrodes that were moved between each pulse through 60° in a plane perpendicular to the long axis of the left hind paws, 30 minutes after an intraperitoneal injection of MTX or saline. We used electrode paste (Gelaid; Nihon Koden, Tokyo, Japan) to prevent skin burns.

Experimental protocol. The animals were assigned to an experimental group or to 1 of 3 control groups, as follows: MTX injection with electroporation (M+/E+ [experimental] group; n = 8), MTX without electroporation (M+/E− group; n = 9), electroporation with saline (M−/E+ group; n = 10), or no treatment (M−/E− group; n = 9).

MTX was provided by Wyeth-Pharmaceutical (Tokyo, Japan). The dose of MTX was set to 0.125 mg/kg body weight, based on preliminary experimental data indicating that no significant systemic antiarthritic changes were recognized at this dose. The drug was administered intraperitoneally twice weekly for 3 weeks, and the animals were killed by asphyxia in carbon dioxide (for radiologic and histologic examination).

These experimental protocols were in accordance with institutional regulations for animal care and were approved by the Institutional Committee for Animal Care of Osaka City University.

Gross inspection and radiologic evaluation. Twice weekly, the animals were weighed using an electronic balance, and hind paw thickness was measured with digital calipers. Three weeks after the adjuvant was injected, the animals were killed using CO_2 asphyxiation, and both hind limbs were harvested and fixed by perfusing cold 4% paraformaldehyde through the left ventricle, followed by immersion in cold 4% paraformaldehyde solution. Soft x-ray images of the hind paws were obtained with a soft x-ray apparatus (DCS-600EX; Aloka, Tokyo, Japan) using settings of 45 kV, 4 mA, and 30 seconds of exposure time. Destructive changes in hind paw bones seen on radiographs were evaluated by criteria previously described by Clark et al (13), with some modifications. Briefly, radiographic

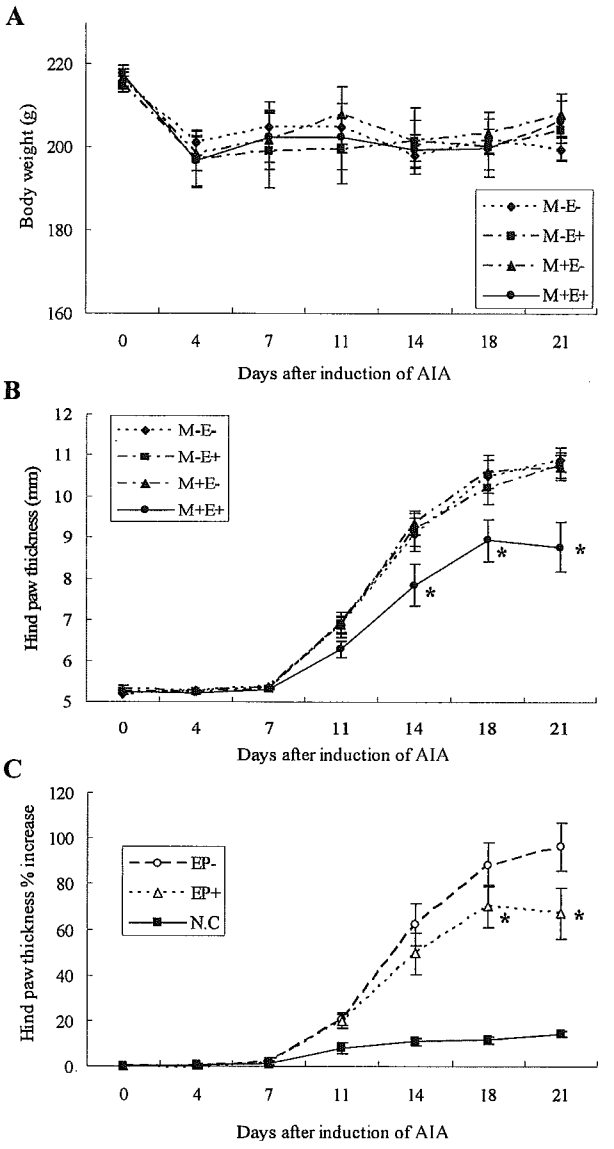

Figure 1. Effects of electrochemotherapy with methotrexate (MTX) on body weight and paw swelling in rats with adjuvant-induced arthritis (AIA). **A,** Weight loss was observed in all groups on day 4. There was no significant weight difference between the 4 groups throughout the entire study period. **B,** Left hind paw thickness, as measured by digital calipers, was maximal on day 21 in the M−/E− (no treatment; n = 9), M−/E+ (electroporation with saline; n = 10), and M+/E− (MTX without electroporation; n = 9) groups. The thickness of the left hind paw treated with electrical pulses after administration of MTX, 0.125 mg/kg/week (M+/E+; n = 8) was significantly decreased when compared with the other groups. * = $P < 0.05$ versus the M−/E−, M−/E+, and M+/E− groups. **C,** Effects of electrical pulses on paw swelling in the M+/E+ group. Electrical pulses were applied to the left hind paw only (electrically treated [EP+]) (n = 8), not the right paw (not electrically treated [EP−]) (n = 8). Application of electrical pulses after administration of low-dose MTX significantly inhibited hind paw swelling on days 18 and 21, as assessed by paw thickness and when compared with EP− paws. NC = negative control (non–adjuvant-injected model) (n = 5). * = $P < 0.05$ versus EP−. Bars show the mean ± SEM.

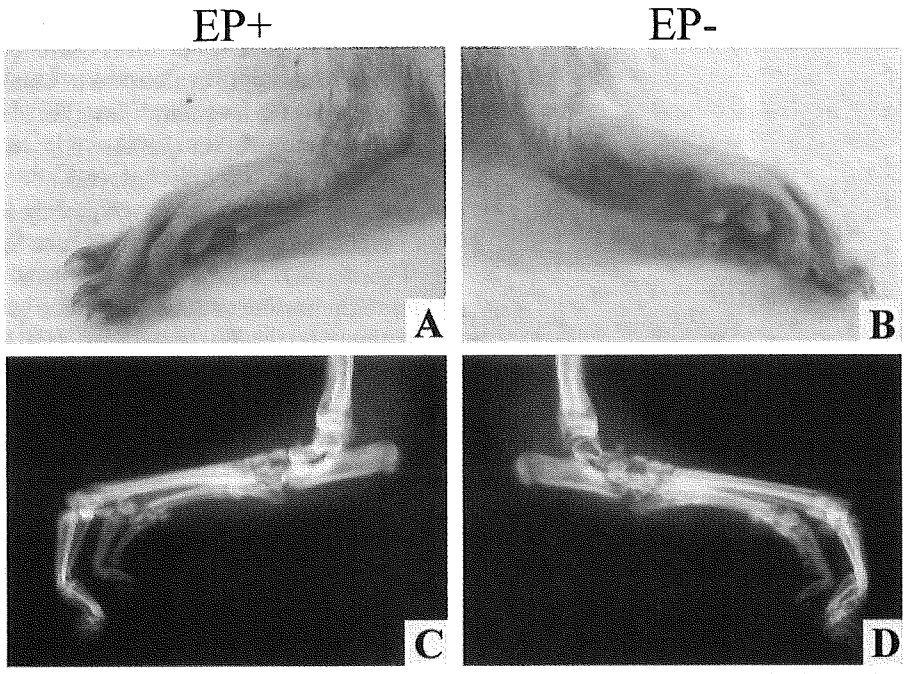

Figure 2. Gross appearance and radiographs of the hind paws of the same rat in the M+/E+ group on day 21. Following administration of MTX (0.125 mg/kg/week), electrical pulses were applied to the left hind paw only (EP+) (**A** and **C**). Note the obvious difference in the degree of swelling and joint damage between the left paw (EP+) and right paw (EP−) in gross appearance (**A** and **B**), as well as on soft x-ray (**C** and **D**). See Figure 1 for definitions.

changes in terms of radiodensity, subchondral bone erosion, periosteal reaction, and cartilage space were evaluated under blinded conditions by 2 rheumatologists (KI and TK) and graded on a 0–3 scale (where 0 = normal and 3 = severely damaged).

Histologic sections. Both hind paws were harvested from the animals for histopathologic examination. After the removal of skin, bones in the hind paws were decalcified in a neutral buffered 14% solution of EDTA/10% formalin, dehydrated in a graded ethanol series, embedded in paraffin, sectioned sagittally into 4-μm sections, and stained with hematoxylin and eosin or toluidine blue. Pathologic changes were evaluated by 2 observers according to a previously reported rating system (14), as follows: grade 0 = normal synovium, cartilage, and bone; grade 1 = hypertrophic synovium with cellular infiltration without pathologic change in bone and cartilage; grade 2 = pannus formation and cartilage erosion in addition to the hypertrophic synovium; grade 3 = additional severe erosion of cartilage and subchondral bone; grade 4 = loss of joint integrity and ankylosis.

In order to identify and count osteoclastic cells, sections were stained for tartrate-resistant acid phosphate (TRAP) using a staining kit (Sigma-Aldrich, St. Louis, MO). TRAP-positive multinucleated cells were counted in 11 selected fields (8 fields in the distal tibia and 3 fields in the talus), all at 100× magnification.

Statistical analysis. Body weight and hind paw thickness were evaluated by repeated analysis of variance and Fisher's protected least significant difference test. Pairwise comparisons were made using Wilcoxon's signed rank tests among groups. All statistical analyses were carried out using StatView software version 5.0 (SAS Institute, Cary, NC). P values less than or equal to 0.05 were considered significant.

RESULTS

Effects of electrochemotherapy on progression of AIA. No significant difference in body weight was noted between the 4 groups during the course of this experiment (Figure 1A), indicating that low-dose MTX, with or without electroporation, had little effect on the systemic physical condition of the rats with AIA.

The thickness of the hind paws in all rats was

Table 1. Radiologic and histologic scores and osteoclast numbers in rat AIA, 21 days after injection of adjuvant*

Group	Radiologic score (n = 8)	Histologic score (n = 8)	Osteoclast number (n = 5)
Right hind paw, EP-negative	3.8 ± 4.5	2.5 ± 1.2	77.6 ± 10.2
Left hind paw, EP-positive†	1.8 ± 2.2	1.3 ± 0.5	22.0 ± 2.4

* Values are the mean ± SD. AIA = adjuvant-induced arthritis; EP = electroporation.
† For all comparisons, $P < 0.05$ versus EP-negative.

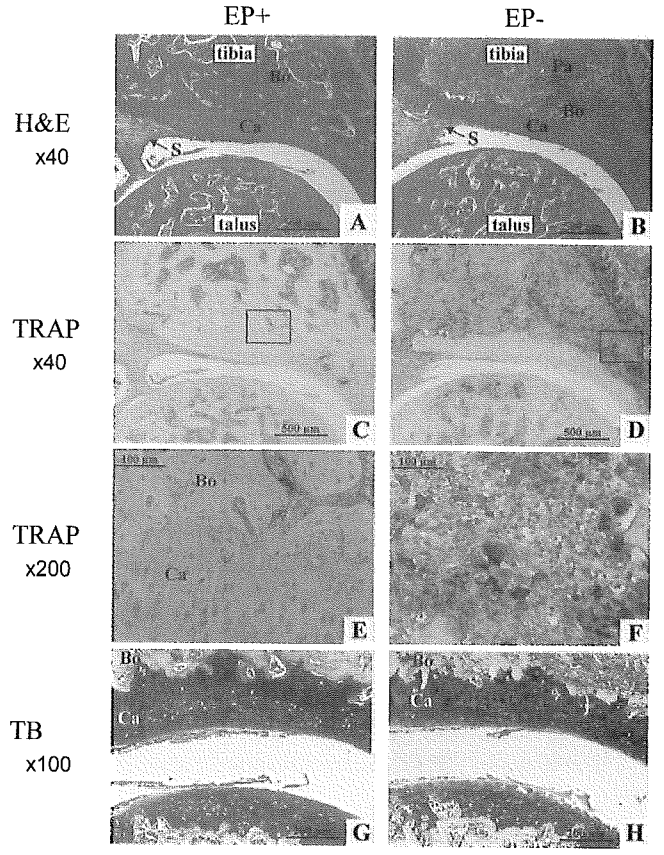

Figure 3. Histologic analysis of the ankle joints of the same rat in the M+/E+ group on day 21. **A** and **B,** Staining with hematoxylin and eosin (H&E). **C, D, E,** and **F,** Staining with tartrate-resistant acid phosphate (TRAP). **G** and **H,** Staining with toluidine blue (TB). The electroporation procedure was applied to the left ankle joint only (EP+) (**A, C, E,** and **G**). No inflammatory synovial tissue erosion into subchondral bone was observed with application of electroporation (**A**) compared with MTX only (**B**). Inflamed synovium infiltrated with lymphocytes was found to contain abundant osteoclastic multinucleated cells on TRAP staining (**D** and **F**). However, there was no difference in metachromasia of articular cartilage in the left and right hind paws. **E,** Higher-magnification view of the boxed area in **C. F,** Higher-magnification view of the boxed area in **D.** Bo = subchondral bone; Ca = cartilage; Pa = pannus; S = synovial tissue (see Figure 1 for other definitions).

significantly and consistently increased from day 11 until the end of the experiment. However, in the M+/E+ group, swelling of the left hind paw was significantly suppressed on days 14, 18, and 21 (Figure 1B) when compared with the 3 control groups (M+/E−, M−/E+, and M−/E−). The gross appearance of the hind paws is shown in Figures 2A and B. Thus, application of electrical pulses appeared to prevent the hind paw joints from progressing to advanced AIA. The degree of swelling differed significantly between the left (electrically treated [EP+]) and right (EP−) paws of the same rat in the M+/E+ group (Figure 1C).

Radiologic evaluation of bones and joints. Radiologic analysis revealed that the hind paw joints were severely damaged in the M−/E−, M−/E+, and M+/E− groups at 21 days after injection of the adjuvant. Therefore, at a dose of 0.125 mg/kg body weight, MTX did not prevent the joint damage (Figure 2D) or local swelling (Figure 2B) caused by progression of arthritis. In contrast, the radiologic damage score was significantly lower in the electrically treated left (EP+) hind paws in the M+/E+ group (Figures 2A and C and Table 1).

Histologic analyses. In the M+/E+ group, the histologic scores were significantly lower in the left hind paws (EP+) than in the right hind paws (EP−) (Figures 3A and B and Table 1). Inflamed synovial tissues with abundant lymphocytes were observed to erode into subchondral bone (Figure 3B). In sections of these joints, the population of TRAP-positive multinucleated osteoclastic cells was significantly lower in the bones of the left hind paw (EP+) than in those of the right hind paw (EP−) (Figures 3C, D, E, and F and Table 1). Toluidine blue staining revealed no degenerative changes of cartilage tissue, including irregularity of articular surface, disorganization of tidemark, and alternation of metachromasia, in either hind paw (Figures 3G and H).

DISCUSSION

These results indicate positive effects of pulsed electrical stimulation for attenuating arthritis by enhancing the antiarthritic effect of MTX. We believe that this is attributable to micropores created by the electrical pulses in the cytoplasmic membranes of cells in the synovium or other inflamed cells. The subsequent passive influx of MTX into the cells would attenuate the inflammatory responses that led to the AIA, although this study did not provide direct evidence of MTX influx. In this preliminary study, we could not identify the cells targeted by electrochemotherapy, and MTX-negative synovial cells, inflammatory cells, or both, may be targets for the drug.

The effects of electrical fields on living cells have been investigated since the 1960s, and high-voltage electrical pulses have been reported to generate transient and reversible pores in cell membranes. This phenomenon has been termed electroporation and is currently used to transfer genes or drugs into cells (6). Electrochemotherapy involves electroporation with drugs, and this methodology is used for the treatment of malignant tumors (5–9). The use of electrochemotherapy to introduce anticancer drugs into malignant tumors has been reported, e.g., bleomycin

for melanoma, basal cell carcinoma, Kaposi's sarcoma, squamous cell carcinoma (6), or chondrosarcoma (15). However, electrochemotherapy with MTX for the treatment of RA has not been reported, although the less-permeable character of MTX and its use as a DMARD in RA would make it an ideal candidate for this approach. Because the effect of pulsed electrical stimulation is expected only at the local site, this method might be applicable for an isolated joint with arthritis that is refractory to systemic chemotherapy or in the early stages of RA involving a limited number of joints without significant joint-destructive changes.

Clinical application of this therapy should not affect normal tissues. Using TUNEL staining, we did not observed any difference in the number of apoptotic cells between the M+/E+ and M+/E− groups (data not shown). We also confirmed in the pilot study that electrical pulses, used under the same conditions as those used in this experiment, did not influence the normal tissues of inbred 9-week-old male Lewis rats. In this pilot study, no inflammatory reactions were observed on histologic examination of the area treated with the electrical pulses, suggesting that electroporation under these conditions did not cause any damage to normal tissue, including cartilage, bone, muscle, and blood vessels (results not shown). However, the clinical application of electrochemotherapy requires further study, including the dose of MTX and the parameters of the electrical pulses.

This experimental study is limited in 2 key areas. First, electrochemotherapy was not applied to joints with established arthritis, and the effect of electrochemotherapy was estimated based on the progression of arthritis. This differs from the clinical situation, in which, as indicated previously (10,11), the inflammatory phase in this AIA model is self-limiting. Therefore, the efficacy of electrochemotherapy for the treatment of established chronic arthritis is difficult to determine in this model. Second, optimization of the application of pulsed electrical current may not be sufficient to obtain maximum delivery of MTX into cells and to achieve maximal antiinflammatory effect in RA. The conditions that enable the efficacy of electrical stimulation in electrochemotherapy may be quite different from the conditions used in the clinical treatment of malignancies that were reference sources for the present study. The potential value of electrochemotherapy for the treatment of RA has been illustrated by these studies, and further work is required to optimize electrochemotherapy to control disease in joints with RA refractory to treatment.

REFERENCES

1. Maini R, St Clair EW, Breedveld F, Furst D, Kalden J, Weisman M, et al, and the ATTRACT Study Group. Infliximab (chimeric anti-tumour necrosis factor α monoclonal antibody) versus placebo in rheumatoid arthritis patients receiving concomitant methotrexate: a randomised phase III trial. Lancet 1999;354:1932–9.
2. Lipsky PE, van der Heijde DM, St Clair EW, Furst DE, Breedveld FC, Kalden JR, et al, and the Anti-Tumor Necrosis Factor Trial in Rheumatoid Arthritis with Concomitant Therapy Study Group. Infliximab and methotrexate in the treatment of rheumatoid arthritis. N Engl J Med 2000;343:1594–602.
3. Furst DE, Kremer JM. Methotrexate in rheumatoid arthritis. Arthritis Rheum 1988;31:305–14.
4. Multicenter evaluation of synovectomy in the treatment of rheumatoid arthritis: report of results at the end of three years. Arthritis Rheum 1977;20:765–71.
5. Heller R, Gilbert R, Jaroszeski MJ. Clinical applications of electrochemotherapy. Adv Drug Deliv Rev 1999;35:119–29.
6. Mir LM, Orlowski S. Mechanisms of electrochemotherapy. Adv Drug Deliv Rev 1999;35:107–18.
7. Hyacinthe M, Jaroszeski MJ, Dang VV, Coppola D, Karl RC, Gilbert RA, et al. Electrically enhanced drug delivery for the treatment of soft tissue sarcoma. Cancer 1999;85:409–17.
8. Horiuchi A, Nikaido T, Mitsushita J, Toki T, Konishi I, Fujii S. Enhancement of antitumor effect of bleomycin by low-voltage in vivo electroporation: a study of human uterine leiomyosarcomas in nude mice. Int J Cancer 2000;88:640–4.
9. Gothelf A, Mir LM, Gehl J. Electrochemotherapy: results of cancer treatment using enhanced delivery of bleomycin by electroporation. Cancer Treat Rev 2003;29:371–87.
10. Welles WL, Silkworth J, Oronsky AL, Kerwar SS, Galivan J. Studies on the effect of low dose methotrexate on rat adjuvant arthritis. J Rheumatol 1985;12:904–6.
11. Kawai S, Nagai K, Nishida S, Sakyo K, Murai E, Mizushima Y. Low-dose pulse methotrexate inhibits articular destruction of adjuvant arthritis in rats. J Pharm Pharmacol 1997;49:213–5.
12. Morgan SL, Baggott JE, Bernreuter WK, Gay RE, Arani R, Alarcon GS. MTX affects inflammation and tissue destruction differently in the rat AA model. J Rheumatol 2001;28:1476–81.
13. Clark RL, Cuttino JT Jr, Anderle SK, Cromartie WJ, Schwab JH. Radiologic analysis of arthritis in rats after systemic injection of streptococcal cell walls. Arthritis Rheum 1979;22:25–35.
14. Shiozawa S, Shimizu K, Tanaka K, Hino K. Studies on the contribution of c-fos/AP-1 to arthritic joint destruction. J Clin Invest 1997;99:1210–6.
15. Shimizu T, Nikaido T, Gomyo H, Yoshimura Y, Horiuchi A, Isobe K, et al. Electrochemotherapy for digital chondrosarcoma. J Orthop Sci 2003;8:248–51.

OsteoArthritis and Cartilage (2005) **13,** 405–417

doi:10.1016/j.joca.2004.12.014

Osteoarthritis and Cartilage | ICRS International Cartilage Repair Society | OA OSTEOARTHRITIS

A new biotechnology for articular cartilage repair: subchondral implantation of a composite of interconnected porous hydroxyapatite, synthetic polymer (PLA-PEG), and bone morphogenetic protein-2 (rhBMP-2)

Noriyuki Tamai M.D., Ph.D.†, Akira Myoui M.D., Ph.D.†, Makoto Hirao M.D.†, Takashi Kaito M.D.†, Takahiro Ochi M.D., Ph.D.‡, Junzo Tanaka Ph.D.§, Kunio Takaoka M.D., Ph.D.‖ and Hideki Yoshikawa M.D., Ph.D.†*

† *Department of Orthopaedic Surgery, Osaka University Graduate School of Medicine, 2-2 Yamadaoka, Suita, Osaka 565-0871, Japan*

‡ *National Hospital Organization Sagamihara National Hospital, 18-1 Sakuradai, Sagamihara, Kanagawa 228-8522, Japan*

§ *Biomaterials Center, National Institute for Materials Science, 1-1 Namiki, Tsukuba, Ibaraki 305-0044, Japan*

‖ *Department of Orthopaedic Surgery, Osaka City University Medical School, 1-4-3 Asahimachi, Abeno-ku, Osaka 545-8585, Japan*

Summary

Objective: Articular cartilage repair remains a major obstacle in tissue engineering. We recently developed a novel tool for articular cartilage repair, consisting of a triple composite of an interconnected porous hydroxyapatite (IP-CHA), recombinant human bone morphogenetic protein-2 (rhBMP-2), and a synthetic biodegradable polymer [poly-D,L-lactic acid/polyethylene glycol (PLA-PEG)] as a carrier for rhBMP-2. In the present study, we evaluated the capacity of the triple composite to induce the regeneration of articular cartilage.

Methods: Full-thickness cartilage defects were created in the trochlear groove of 52 New Zealand White rabbits. Sixteen defects were filled with the bone morphogenetic protein (BMP)/PLA–PEG/IP-CHA composite (group I), 12 with PLA–PEG/IP-CHA (group II), 12 with IP-CHA alone (group III), and 12 were left empty (group IV). The animals were killed 1, 3, and 6 weeks after surgery, and the gross appearance of the defect sites was assessed. The harvested tissues were examined radiographically and histologically.

Results: One week after implantation with the BMP/PLA–PEG/IP-CHA composite (group I), vigorous repair had occurred in the subchondral defect. It contained an agglomeration of mesenchymal cells which had migrated from the surrounding bone marrow either directly, or indirectly via the interconnecting pores of the IP-CHA scaffold. At 6 weeks, these defects were completely repaired. The regenerated cartilage manifested a hyaline-like appearance, with a mature matrix and a columnar organization of chondrocytes.

Conclusions: The triple composite of rhBMP-2, PLA-PEG, and IP-CHA promotes the repair of full-thickness articular cartilage defects within as short a period as 3 weeks in the rabbit model. Hence, this novel cell-free implant biotechnology could mark a new development in the field of articular cartilage repair.

Key words: Articular cartilage repair, Interconnected porous hydroxyapatite (IP-CHA), BMP, PLA-PEG.

Introduction

To date, the myth "once destroyed, cartilage cannot be repaired" has yet to be dispelled[1]. Mature articular cartilage cannot heal spontaneously owing to its low mitotic activity, which contrasts to the rapid rate of chondrocytic mitosis during normal cartilage growth.

Recently, several researchers have attempted to utilize culture-expanded autologous chondrocytes in combination with collagen sponges or fibrin glue to effect the repair of cartilage defects[2,3]. However, the results were either unsatisfactory or, if satisfactory, were achieved only after a lengthy wait for the regeneration of hyaline cartilage[2,4]. These poor results may reflect the characteristics of the transplantation technique, which involves the application of cartilage-derived cells to the defect[5].

Mesenchymal stem cells (MSCs) isolated from bone marrow have the ability to differentiate into chondrocytes, osteoblasts and other connective tissue cells of mesenchymal origin when cultured under appropriate *in vitro* conditions[6,7]. In an effort to exploit the pluripotentiality of MSCs, MSC-based repair strategies have been instigated in rabbits and goats, but with limited success[8,9]. Clinically,

*Address correspondence and reprint requests to: Hideki Yoshikawa. Tel: 81-6-6879-3552; Fax: 81-6-6879-3559; E-mail: yhideki@ort.med.osaka-u.ac.jp
Received 8 November 2004; revision accepted 20 December 2004.

surgical interventions, such as microfracturing, abrasion arthroplasty and osteochondral drilling, have been widely used and considered to be partially successful[10,11]. These techniques are based on the concept that intentional damage to the subchondral bone recruits MSCs to the defect, thereby promoting cartilage repair.

A potentially powerful alternative approach for cartilage regeneration is the local administration of bone morphogenetic proteins (BMPs), which are members of the transforming growth factor-β superfamily. BMPs have been shown to regulate and promote the growth and differentiation of chondrocytes, osteoblasts and MSCs[12,13]. Indeed, recombinant human bone morphogenetic protein-2 (rhBMP-2) can stimulate the *in vitro* synthesis of components of the chondrocytic matrix, such as proteoglycans and type-II collagen[14–16]. Furthermore, BMPs are known to induce the condensation of MSCs when administered *in vivo*[17–19].

Inorganic biomaterials, such as carbon fibers[20], collagen scaffolds[2,21], absorbable polymers[22,23], and hydroxyapatite[24,25], have been used for articular cartilage repair. Some success has been achieved in the repair of small osteochondral defects, but no widely accepted method exists for the complete healing of hyaline cartilage. The cause of the failure lies not in the nature of the biomaterial itself but in its structure, which is not regulated three-dimensionally.

In the present study, we attempted to combine two distinct approaches: the strong induction of subchondral bone regeneration, with a view to recruiting bone-marrow MSCs to the osteochondral defect; and the appropriate local delivery of rhBMP-2 to induce chondrocytic differentiation and to stimulate matrix production by the chondrocytes. To instigate these two approaches simultaneously, we developed a combined biomaterial, which consists of a synthetic hydroxyapatite with an interconnected porous structure (IP-CHA), and a synthetic bioabsorbable polymer, namely, PLA–PEG (poly-D,L-lactic acid–polyethylene glycol block copolymer). In this system, PLA–PEG serves as a drug-delivery carrier, which permits the ideal release of rhBMP-2 over a period of about 3 weeks[26–29]. IP-CHA is made from hydroxyapatite, which is a bioactive ceramic with osteoconductive properties[30,31]. In addition, IP-CHA has a finely organized, three-dimensional interconnecting pore structure. The material is highly porous (porosity: 75%) and the pore size (150 μm) is appropriate for bone formation. The large interconnecting channels (average diameter: 40 μm) permit the easy penetration of tissue into the deep pores[30]. Owing to these structural properties, IP-CHA can itself induce local bone repair processes[30,32,33]. The interconnecting pore structure of the material also permits its easy impregnation with cytokines or growth factors borne by an appropriate delivery system.

The rationale behind the selection of key experimental design parameters was as follows: Skeletally immature adolescent rabbits (4–6 months old and 2.5–3.0 kg in weight) were selected because the ability of articular cartilage to repair depends mostly on the bone-marrow MSCs, which are metabolically more active and have a higher capacity to induce repair in an immature model. The decision to use full-thickness defects with a diameter of 4 mm and a depth of 6 mm was based on the results of previous studies. In rabbits, partial-thickness defects do not heal spontaneously, whereas full-thickness ones with a diameter less than 3 mm do, and the repair tissue is composed either of hyaline- or of fibrocartilage[34–36]. Hence, it was necessary to establish a model in which this upper limit for spontaneous repair was exceeded.

In the present study, we demonstrate the capacity of the triple composite of rhBMP-2, PLA-PEG, and IP-CHA to effect articular cartilage repair. The goal was to achieve the repair of full-thickness articular cartilage defects in rabbits in as short a time as possible, with the ultimate view of inducing the repair of similar lesions in humans; specifically, those generated during osteoarthritis, rheumatoid arthritis, and osteochondritis dissecans.

Materials and methods

PREPARATION OF IMPLANTS

IP-CHA was synthesized by Toshiba Ceramics Co., Ltd. (Kanagawa, Japan), as previously described[30]. In short, we adopted a "foam gel" technique, which involves two unique steps: a foaming step and a crosslinking step. During the foaming step, the hydroxyapatite slurry is mixed with a foaming agent (polyethyleneimine, 40% by weight). During the crosslinking (polymerization) step, the foam-like hydroxyapatite slurry is rapidly gelatinized using a water-soluble crosslinking agent (a poly-functional epoxy compound)[30].

rhBMP-2, which is produced by the Genetics Institute (Cambridge, MA) and was given to us by Yamanouchi Pharmaceutical Co., Ltd. (Ibaraki, Japan), was dissolved in buffer (5 mM glutamic acid, 2.5% glycine, 0.5% sucrose, and 0.01% Tween 80) at a concentration of 1 mg/ml. The solution was then filter-sterilized. Two-hundred mg of PLA–PEG [molecular weight (MW) = 11,400, dispersity (Mw/Mn) = 1.1 (Taki Chemical Research Laboratory, Kanagawa, Japan)] was dissolved in 1 ml of acetone. To prepare a single implant sample, a 25 μl aliquot of the PLA–PEG mass (5 mg) was mixed with a 20 μl sample of rhBMP-2 (20 μg). The specimen of IP-CHA (4 mm in diameter and 4 mm in height) was immersed in the mixture and the solvent was evaporated in a centrifuge/evaporator. The resulting BMP/PLA–PEG/IP-CHA composite was sterilized with ethylene oxide gas for 24 h on the day preceding implantation.

IN VITRO RELEASE KINETICS OF RHBMP-2

The release of rhBMP-2 from the BMP/PLA–PEG/IP-CHA composite was measured using a quantitative sandwich enzyme immunoassay technique (AN'ALYZA®; BMP-2 immunoassay, TECHNE Co. MN, USA). The dose of rhBMP-2 used in the *in vivo* experiments (20 μg) was chosen for the release study. Twelve BMP/PLA–PEG/IP-CHA composites, which were prepared in the same way as those used for implantation in the rabbit model, were placed within 24-well plates together with 500 μl of phosphate-buffered saline [(PBS) Sigma] and incubated for 21 days at 37°C. The supernatant was removed and replaced with fresh PBS every day. The supernatants removed on days 1, 3, 7, 14 and 21 were analyzed for their concentrations of rhBMP-2 according to the enzyme-linked immunosorbent assay (ELISA) technique. The bioactivity of the composites maintained *in vitro* for 0, 7 and 21 days (four samples per time point) was also assessed (see next section).

IN VIVO BIOASSAY FOR THE BMP/PLA–PEG/IP-CHA COMPOSITE

To assess the biological activity of composites that were maintained *in vitro* for 0, 7 and 21 days, these, as well as

IP-CHAs without rhBMP-2 (controls), were implanted within the back muscles of 5-week-old male JCL: ICR mice (one composite per animal; four mice per group, i.e., control, day 1, day 7 and day 21) as previously reported[27,28]. The implants were harvested 2 weeks after implantation. They were then crushed, homogenized in 0.2% Nonidet P-40 containing 1 mM $MgCl_2$, and centrifuged at 10,000 rpm for 1 min at 4°C. The supernatants were assayed for alkaline phosphatase (ALP) activity using *p*-nitrophenyl phosphate as a substrate. The product was measured spectrophotometrically at an absorption wavelength of 410 nm ($n = 4$ per group)[37].

ANIMAL EXPERIMENTS

Fifty-two New Zealand White rabbits weighing 2.5–3.0 kg (4–6 months) were kept in cages and had free access to food pellets and water. The rabbits were anesthetized by the intravenous injection of 1 ml of pentobarbital [50 mg/ml (Nembutal®; Dainippon Pharmaceutical Co. Ltd., Osaka, Japan)] and the intramuscular injection of 1 ml of xylazine hydrochloride [25 mg/ml (Seractal®; Bayer, Germany)]. After shaving, disinfection, and draping, a straight 3-cm long medial parapatellar incision was made over the right knee and the patella was everted. Full-thickness articular osteochondral defects, 4 mm in diameter and 6 mm in depth, were created mechanically in the patellar groove of the right distal femur. Rabbit knees were divided into four implant groups: group I ($n = 16$ knees) received the BMP/PLA–PEG/IP-CHA composite; group II ($n = 12$ knees) received the PLA–PEG/IP-CHA composite (no rhBMP-2), group III ($n = 12$ knees) received IP-CHA alone; and group IV ($n = 12$ knees) underwent a sham operation with no implantation. In groups I, II, and III, all implants were placed at the subchondral bone level, 2 mm beneath the surface of the adjacent cartilage. The fascial layer was closed with absorbable sutures, and the skin with 4-0 nylon sutures. One week after surgery, four rabbits in group I were killed. At 3 weeks, 24 rabbits were killed (group I = 6, group II = 6, group III = 6, group IV = 6), and at 6 weeks 24 rabbits were killed (group I = 6, group II = 6, group III = 6, group IV = 6). The animals were killed by an intravenous injection of 5 ml of pentobarbital (Table I). All animal experiments were approved by the Animal Laboratory, Faculty of Medicine, Osaka University, Japan.

RADIOGRAPHIC AND HISTOLOGICAL EVALUATIONS

The harvested tissues were radiographed using a soft X-ray apparatus [35 kV; 300 μA; 300 s; MX20 (Faxitron X-ray Co., IL, USA)] and then fixed in 4% paraformaldehyde (pH 7.4) for 48 h at 4°C. Tissue samples were decalcified in 20% ethylenediaminetetraacetic acid (pH 7.4) at 4°C, dehydrated in a graded ethanol series and embedded in paraffin. Serial sections (5 μm in thickness) were cut sagittally through the center of the operative site and stained with hematoxylin and eosin (H&E) or with safranin-O. For the immunohistochemical analysis, paraffin sections were treated with 3% H_2O_2 to block endogenous peroxidase activity. They were pretreated with serum to block non-specific staining. The sections were then incubated with mouse monoclonal antibodies: anti-type-I collagen (I-8H5, Daiichi Fine Chemical Co., Ltd, Toyama, Japan), anti-type-II collagen (II-4C11, Daiichi Fine Chemical Co., Ltd, Toyama, Japan), and anti-CD105 [(Endoglin) 555722, BD Bioscience, NJ, USA]; and with the polyclonal antibody goat anti-Cbfa1 [(Runx2) C-19, Santa Cruz, CA, USA][38]. The specimens were treated with the appropriate biotinylated secondary antibodies, and then incubated with the streptavidin/horseradish peroxidase complex. The signal was visualized as the red reaction product of a 3-amino-9-ethyl carbazole liquid substrate chromogen (AEC, DAKO JAPAN Co., Ltd, Kyoto, Japan). To confirm the specificity of

Table I
Information respecting the deployment of the 52 rabbits used in this study

	Number of rabbits				Total number
	Group I	Group II	Group III	Group IV	
Materials					
IP-CHA	+	+	+	–	
rhBMP-2	+	–	–	–	
PLA–PEG	+	+	–	–	
Follow-up time					
1 week	4	0	0	0	4
3 weeks	6	6	6	6	24
6 weeks	6	6	6	6	24
Total number	16	12	12	12	52

Table II
*Histological scoring system**

Category	Points
Cell morphology	
Hyaline cartilage	4
Mostly hyaline cartilage	3
Mostly fibrocartilage	2
Mostly non-cartilage	1
Non-cartilage only	0
Matrix-staining (metachromasia)	
Normal	3
Slightly reduced	2
Markedly reduced	1
No metachromatic staining	0
Structural integrity	
Normal	2
Slight disruption	1
Severe disintegration	0
Surface regularity†	
Smooth	3
Moderate	2
Irregular	1
Severely irregular	0
Thickness of cartilage, %	
121–150	1
81–120	2
51–80	1
0–50	0
Regenerated subchondral bone	
Good	2
Moderate	1
Poor	0
Integration with adjacent cartilage	
Both edges integrated	2
One edge integrated	1
Neither edge integrated	0
Total maximum	18

*A modified version of the system described by Wakitani *et al.*[8].

†Total smooth area of repair cartilage compared with the entire area of the cartilaginous compartment of the defect.

the antibody under the adopted conditions and to confirm the specificity of the markers in target cells, all antibodies were tested for their reactivity in control tissues.

HISTOLOGICAL SCORING

To quantify the histological repair of articular cartilage defects, we employed a modified version of the grading scale described by Wakitani *et al.*[8]. This consists of seven categories and assigns a score ranging from 0 to 18 points (Table II). The following parameters were assessed: cell morphology (hyaline cartilage); metachromatic staining of the cartilage matrix; structural integrity of the regenerated cartilage; surface regularity of the tissue; thickness of the cartilage layer; regeneration of the subchondral bone; and integration of the tissue with adjacent cartilage.

STATISTICAL ANALYSES

Data pertaining to ALP activity were analyzed using an unpaired Student's *t* test. The histological scoring data were analyzed using the Kruskal–Wallis test, with a *post hoc* Bonferroni correction for non-parametric data.

Results

EVALUATION OF THE IMPLANTS

Scanning electron microscopy of IP-CHA samples revealed these to have a finely organized three-dimensional structure. Most of the IP-CHA pores were spherical, of similar size (approximately 100–200 μm in diameter) and uniformly interconnected via channels [10–80 μm in diameter; Fig. 1(B, C)]. Scanning electron microscopy of the BMP/PLA–PEG/IP-CHA composite revealed the BMP/PLA–PEG component to affect neither the pore size nor the interconnecting pore structure and to coat well the surface of the IP-CHA [Fig. 1(D, E)].

IN VITRO RELEASE KINETICS OF RHBMP-2 AND *IN VIVO* BIOASSAY FOR THE BMP/PLA–PEG/IP-CHA COMPOSITE

Based on ELISA, the BMP/PLA–PEG/IP-CHA composite released significant quantities of rhBMP-2 during the 21-day monitoring period [6.85 ± 1.31 μg/ml on day 1, 0.79 ± 0.22 μg/ml on day 3, 22.9 ± 0.62 ng/ml on day 7, 4.76 ± 1.13 ng/ml on day 14, and 2.71 ± 0.70 ng/ml on day 21; Fig. 2(A)].

To assess the bioactivity of the BMP/PLA–PEG/IP-CHA composites maintained *in vitro* for 0, 7 or 21 days, we implanted these, as well as IP-CHAs (control for the absence of rhBMP-2) within the back muscles of male ICR mice (a standard ectopic bone-formation model) and then analyzed the explanted material for its ALP activity. High levels of ALP activity could be detected even on day 21 [Fig. 2(B)], which accords with the rhBMP-2 release kinetics results *in vitro*.

MACROSCOPIC OBSERVATIONS OF CARTILAGE DEFECTS

Three weeks after implantation, the repaired defects in group I had a macroscopically smooth and glistening appearance and exhibited continuity with the surrounding host cartilage [Fig. 3(A)]. The controls (groups II–IV) revealed varying degrees of cartilage resurfacing with fibrous tissue [Fig. 3(B–D)].

At 6 weeks, the color and the glistening appearance of the repaired defects in group I were similar to those manifested by the adjacent host cartilage. The junction between the repaired tissue and the surrounding host cartilage was not clearly visible [Fig. 3(E)]. In contrast, the regenerated tissue in the control groups (groups II–IV) was

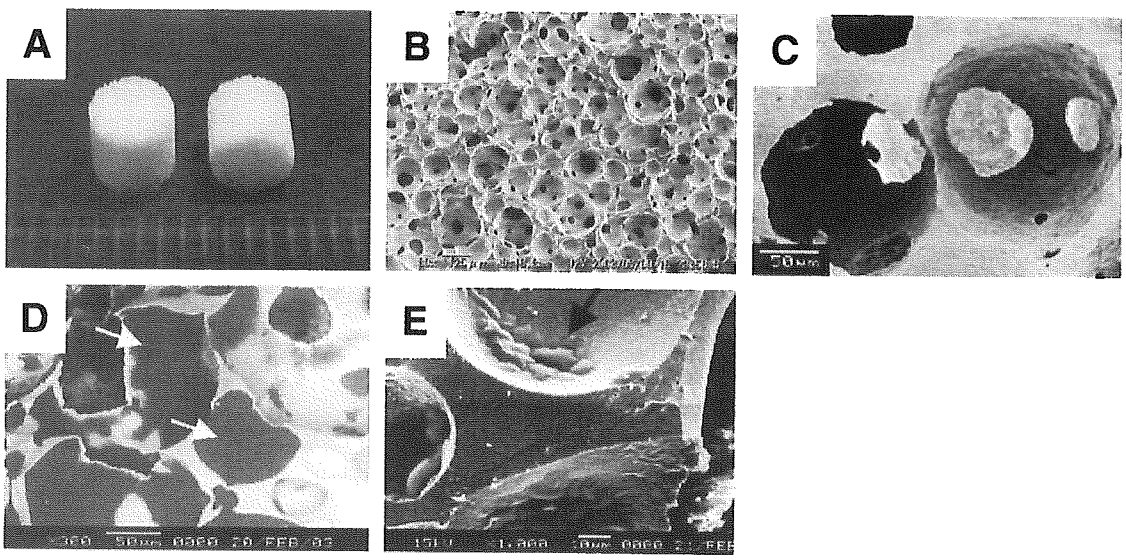

Fig. 1. Macroscopic photograph (A) and scanning electron micrographs (B–E) of IP-CHA specimens (4 mm in diameter and 4 mm in height). (A) Macroscopically, the surface of IP-CHA is slightly rough compared with that of other commercial porous hydroxyapatite materials, owing to its regular porous structure. (B, C) Scanning electron micrographs of IP-CHA, illustrating the regular arrangement of pores which are of similar size (100–200 μm in diameter), uniformly connected with each other, and separated by thin walls. (B) = 80×; (C) = 600×. (D, E) Scanning electron micrographs of the BMP/PLA–PEG/IP-CHA composite. (D) The dark areas lining the pores (white arrows) represent the BMP/PLA–PEG component. The introduction of BMP/PLA–PEG had no effect on either the pore size or the interconnecting pore structure. (E) Higher magnification of the lining of a pore (black arrow), revealing it to be well coated with BMP/PLA–PEG. (D) = 300×; (E) = 1000×.

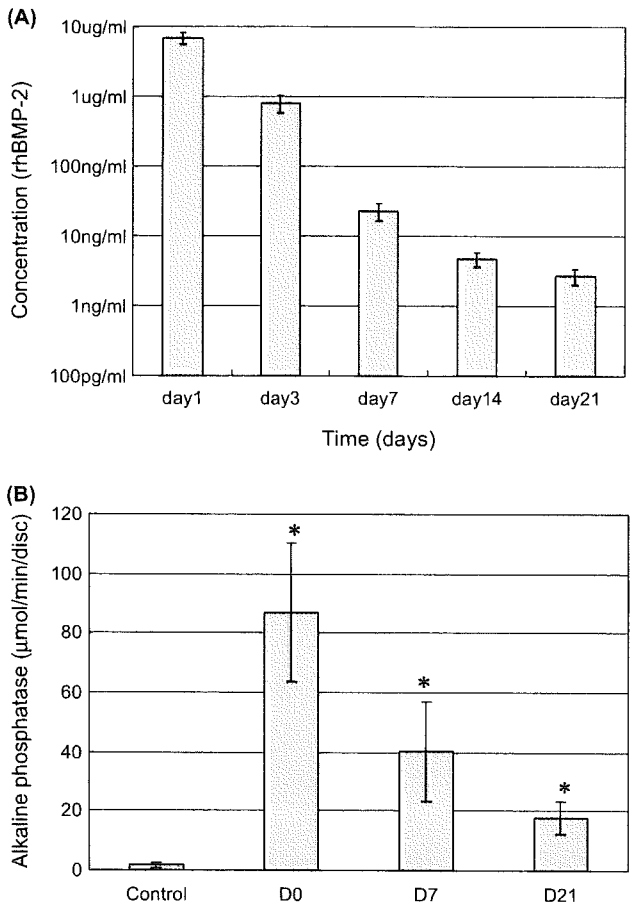

Fig. 2. Time course of rhBMP-2 release from the BMP/PLA–PEG/IP-CHA composite *in vitro* (A) and the bioactivity of the composites *in vivo* (B). (A) Release kinetics (measured by ELISA) of rhBMP-2 from the BMP/PLA–PEG/IP-CHA composite, illustrating significant quantities of rhBMP-2 during the 21-day monitoring period. The bar graph depicts the non-cumulative release at each time point. Mean values ± SD ($n = 4$) are represented. (B) The bioactivity of BMP/PLA–PEG/IP-CHA composites that were maintained *in vitro* for 0 (D0), 7 (D7), or 21 (D21) days was assessed 2 weeks after their implantation at an ectopic site in mice by monitoring the ALP activity of the explanted material. PLA–PEG/IP-CHA (no rhBMP-2) represented the control. High levels of ALP activity could be detected even on day 21 [86.8 ± 23.2 μmol/min/disc (day 0), 40.3 ± 16.8 μmol/min/disc (day 7), 17.7 ± 5.2 μmol/min/disc (day 21), 1.6 ± 0.8 μmol/min/disc (control)]. Mean values ± SD ($n = 4$) are represented. * = value is significantly different from the control ($P < 0.05$).

fibrous, and had a rough surface containing many fissures [Fig. 3(F–H)].

RADIOGRAPHIC EVALUATION

Six weeks after implantation, the soft X-ray analysis revealed defects treated with the BMP/PLA–PEG/IP-CHA composite (group I) to be consistently filled with newly formed bone, which was continuous with the surrounding intact subchondral bone [Fig. 3(I)]. In the control groups (groups II–IV), bone formation was incomplete and irregular [Fig. 3(J–L)].

HISTOLOGICAL EVALUATION

One week after implantation with the BMP/PLA–PEG/IP-CHA composite (group I), vigorous new bone formation was observed histologically within the pores of the IP-CHA scaffold [Fig. 4(B)], and about three-quarters of the defect depth above the IP-CHA had already been replaced with repair tissue. The central part of the repair tissue contained a fibrin clot and a few vessels. The lateral and lower regions consisted of granulation tissue, which was actively undergoing neovascularization and contained rounded fibroblast-like cells. These cells registered positive for Cbfa1 and/or CD105. They appeared to have infiltrated from the surrounding intact subchondral bone, either directly, or indirectly via the interconnecting IP-CHA pores, which were likewise filled with granulation tissue. Some of the pores in the peripheral 1-mm portions of IP-CHA blocks already contained newly formed bone (Fig. 4).

Three weeks after implantation with BMP/PLA–PEG/IP-CHA, the defect space above the IP-CHA blocks (subchondral space) was filled with newly generated and vigorous bone tissue, which penetrated the interconnecting pores of this material [Fig. 5(A, F)]. The regenerated articular cartilage was more cellular and contained less extracellular matrix than normal cartilage. The regenerated cartilage was divided into three distinct zones: (1) a superficial one, which contained flattened hyperchromatic cells; (2) a middle one, which contained rounded chondrocytes; and (3) a zone of enchondral ossification. The cartilage-like layer was two-to-three times thicker than normal cartilage [Fig. 5(A, E)]. In each of the control groups (groups II–IV), the regenerated fibrous cartilage had a similar morphological appearance, irrespective of the absence or presence of an implant. Although the subchondral space in group II tended to be filled with more newly formed bone than did that in the other control groups (groups III and IV), the quantitative histological evaluation revealed no significant difference between them [Table III; Fig. 5(B–D)].

Six weeks after implantation, defects treated with the BMP/PLA–PEG/IP-CHA composite (group I) were filled with regenerated subchondral bone, which also penetrated the pores of the implant. The subchondral bone was covered with a layer of regenerated cartilage tissue of almost normal thickness. The hyaline nature of the cartilage was maintained, and the tissue was beginning to assume a columnar organization and a horizontal stratification into four distinct zones (superficial, middle, deep and calcified), as in normal cartilage [Fig. 6(A, E)]. Interestingly, no gaps could be distinguished microscopically between the host cartilage and the newly regenerated cartilage, which suggests that the tissues were functionally and biologically integrated [Fig. 6(F)]. Safranin-O staining was evident predominantly in the middle and deep zones. Immunoreactivity for type-II collagen tended to be weakest in the deep zone at the junction with host tissue. But generally, the matrix exhibited a hyaline-like cartilaginous phenotype [registering negative for type-I collagen; Fig. 6(J–L)]. In contrast, defects in the control groups (groups II–IV) were filled with a hypercellular type of fibrous tissue. No hyaline cartilage was detected, despite the presence of new bone above and within the implant; [Fig. 6(B–D, G–I)]. Histological sections were assessed quantitatively using a modified version of an established grading system, which measures the degree and quality of cartilage repair[8] (Table II). At each time point, the scores for the BMP/PLA–PEG/IP-CHA composite (group I) were significantly better than those for groups II, III and IV ($P < 0.01$). These findings accord with the macroscopic and histological observations.